Characterization of habitable Exoplanets with simultaneous Coronagraphy and Astrometry with a single Aperture Telescope

Olivier Guyon*[a,b,c], Eduardo Bendek[c], S. Mark Ammons[d], Michael Shao[e], Stuart Shaklan[e], Robert A. Woodruff, Ruslan Belikov[f], Thomas Milster[c]

[a]Steward Observatory, University of Arizona, 933 Cherry Ave., Tucson, AZ 85721, USA;
[b]Subaru Telescope, National Astronomical Observatory of Japan, 650 N. A'ohoku Place, Hilo, HI 96720, USA;
[c]College of Optical Sciences, University of Arizona, Tucson, AZ 85721, USA;
[d]Lawrence Livermore National Laboratory, Physics Division L-210, CA 94550, USA;
[e]Jet Propulsion Laboratory, 4800 Oak Grove Drive, Pasadena, CA 91109, USA;
[f]NASA Ames Research Center, Moffet Field, Mountain View, CA, USA

ABSTRACT

With sub-microarcsecond astrometry, exoplanets can be identified and their masses measured. Coronagraphic imaging of these exoplanets is required to study their atmospheres and surfaces in sufficient detail to identify possible signs of biological activity. We show how both measurements can be simultaneously acquired with a single telescope in which the central field is directed to a coronagraph instrument providing high contrast images, while the surrounding field is imaged with a wide field camera in which numerous faint background stars are used as an astrometric reference. To calibrate astrometric distortions due to optics and focal plane detector array imperfections and variations, we propose to place small dark spots on the telescope primary mirror. The spots, arranged in a regular grid containing no low spatial frequencies, do not affect the coronagraph performance. In the wide field image, they create diffraction spikes originating from the central bright star, which are affected by changes in intrumental distortions in exactly the same way as the background stars used for reference, thus allowing calibration of instrumental errors to micro-arcsecond level. We show that combining simultaneous astrometric and coronagraphic measurements allows reliable detection and characterization of exoplanets. Recent laboratory tests performed at the University of Arizona and NASA Ames validate the concept, demonstrating both the ability to accurately calibrate astrometric distortions, and compatibility with high contrast imaging systems.

Keywords: Astrometry, Exoplanets, Coronagraphy

1. INTRODUCTION

Among the existing techniques to identify exoplanets, astrometry and direct imaging are particularly well suited for identification and characterization of nearby habitable planets. Either technique can provide a full census of habitable planets around nearby (approximately d < 10pc) F,G,K main sequence stars, provided that it achieves the required sensitivity (sub-μas single measurement precision for astrometry, 1e−9 raw contrast at ≈ 100mas for coronagraphy). Extensive characterization of the exoplanet does however require both techniques, which provide complementary information (mass vs orbit and spectra). This paper describes how both measurements can be acquired simultaneoulsy with a single wide field telescope using the diffractive pupil telescope concept[1]. We provide an overview of its benefits and its expected astrometric performance. Early results from laboratory demonstration of the concept are described in a separate publication[2].

*guyon@naoj.org; phone 1 818 293 8826

2. ASTROMETRIC MEASUREMENT WITH A WIDE FIELD TELESCOPE

2.1 Principle

The astrometric measurement is performed from a wide field image around the target, in which the numerous background stars are used as the astrometric reference. With a field of view of about one tenth of a square degree or more, the background stars, even for a galactic pole pointing, are sufficiently numerous and bright to theoretically offer sub-μas measurement precision in a few hours exposure: the challenge in obtaining a high accuracy astrometric measurement is to overcome optical distortions and detector defects.

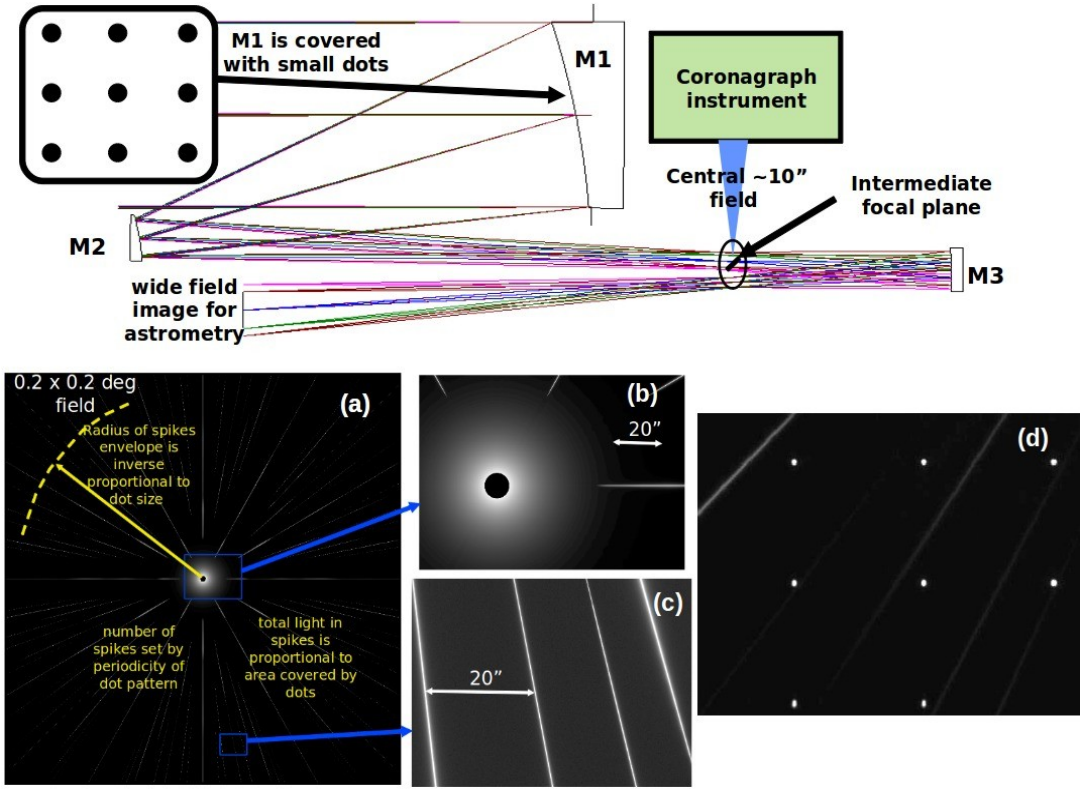

Figure 1. Conceptual optical design for the diffractive pupil telescope (DTP). The top part of this figure shows how light is shared between two instruments. The central field containing the bright star and its immediate surroundings is extracted at the telescopeâ€™s intermediate focus and fed to a coronagraph instrument for high contrast imaging. The wide well-corrected outer field is imaged onto a large focal plane detector array. Panels (a) to (d) show details of the wide field image acquired in the final focal plane. (a) The wide-field image shows the diffraction spikes introduced by the dots on the primary mirror. (b) The central part of the target image, containing most of the flux, is missing from the wide-field image as it has been directed to the coronagraph instrument. (c) Faint diffraction spikes pave the rest of the field. (d) Faint background stars are imaged simultaneously with the diffraction spikes. While images (a) to (c) are simulated, image (d) was acquired in a laboratory demonstration of the technique..

The proposed astrometric measurement principle is illustrated in figure 1, showing a single aperture telescope equiped with two instruments: a narrow field high contrast imaging instrument to directly image and characterize (spectroscopy) exoplanets, and a wide field camera that can be used for the astrometric measurement. Thanks to a regular grid of small dots uniformly covering about 1% of the primary mirror area, diffraction spikes that encode the central star position are created in the wide field image. This concept simultaneously addresses two fundamental challenges for the astrometric measurement:

Flux contrast between the bright central star and the faint background stars: the astrometric measurement is performed between diffraction spikes of the central target and faint background stars – both features have similar surface brightness in the image

Optical distortions in a wide field imaging system: While such distortions are inevitably orders of magnitudes larger than the uas-level astrometric accuracy seeked, the diffraction spikes and the background stars experience the same distortions. This error term is therefore (mostly) removed from the measurement. This point is discussed in more detail in the following sections.

2.2 Data acquisiton and analysis

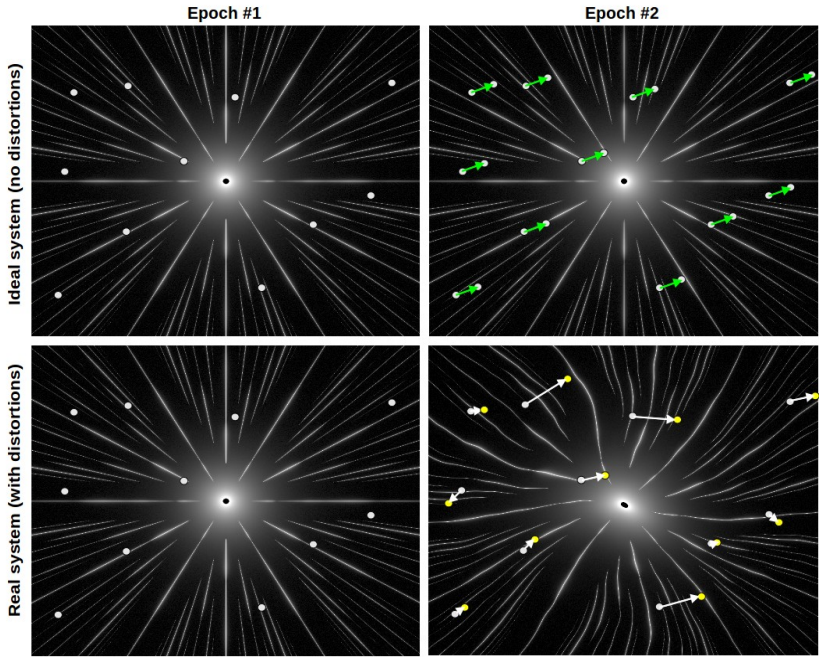

Figure 2. Data acquisition with the DPT technique. See text for details.

The astrometric measurement is illustrated in figure 2, which shows how the wide field images should appear in an ideal system free of distortions (top row). The same target star is observed at two epochs, and its astrometric motion on the sky is measured between the two observations as an apparent displacement of the background stars (green vectors in the top right image). Note that the central star is missing from this image, as the central field is fed to the coronagraph instrument. The astrometric motion can in this case be obtained by averaging all the green vectors. In the presence of distortions (bottom row), distortions due to changes in optical surface changes and focal plane array motion are added to the astrometric signal. This noise is much larger than the uas-level measurement accuracy required. The distortion component can be measured by comparing the diffraction spikes position between the two epochs, and a map of the distortion change between the two epochs can thus be built. This map can only be established with good precision in the angular direction, due to the strongly elongated shape of the spikes. Once this map is computed, it is subtracted from the astrometric motion measured for the background stars to yield a distortion-free measurement.

Table 1. Main error terms in wide field imaging for astrometry, and corresponding solution/mitigation strategy.

Error term	Solution / mitigation
Optical and detector distortions, low order	Calibrated with diffraction spikes
Optical and detector distortions, high order	Averaged over telescope roll and large number of background stars
Pixel defects	Averaged by telescope roll and large number of background stars
Astrophysical noise on background stars (planets, binaries)	Averaged by large number of background stars. Most stars are faint and distant Halo stars. Binaries can be identified by relative astrometry between background stars

In addition to the calibration described above, the telescope is slowly rolled during the measurement to average detector pixel defects well below the μas level. Table 1 summarizes how the propose technique addresses the main sources of astrometric measurement noise, excluding photon noise and detector readout noise.

3. ASTROMETRIC PRECISION

3.1 Astrometric Precision with a 1.4 m Telescope: numerical model

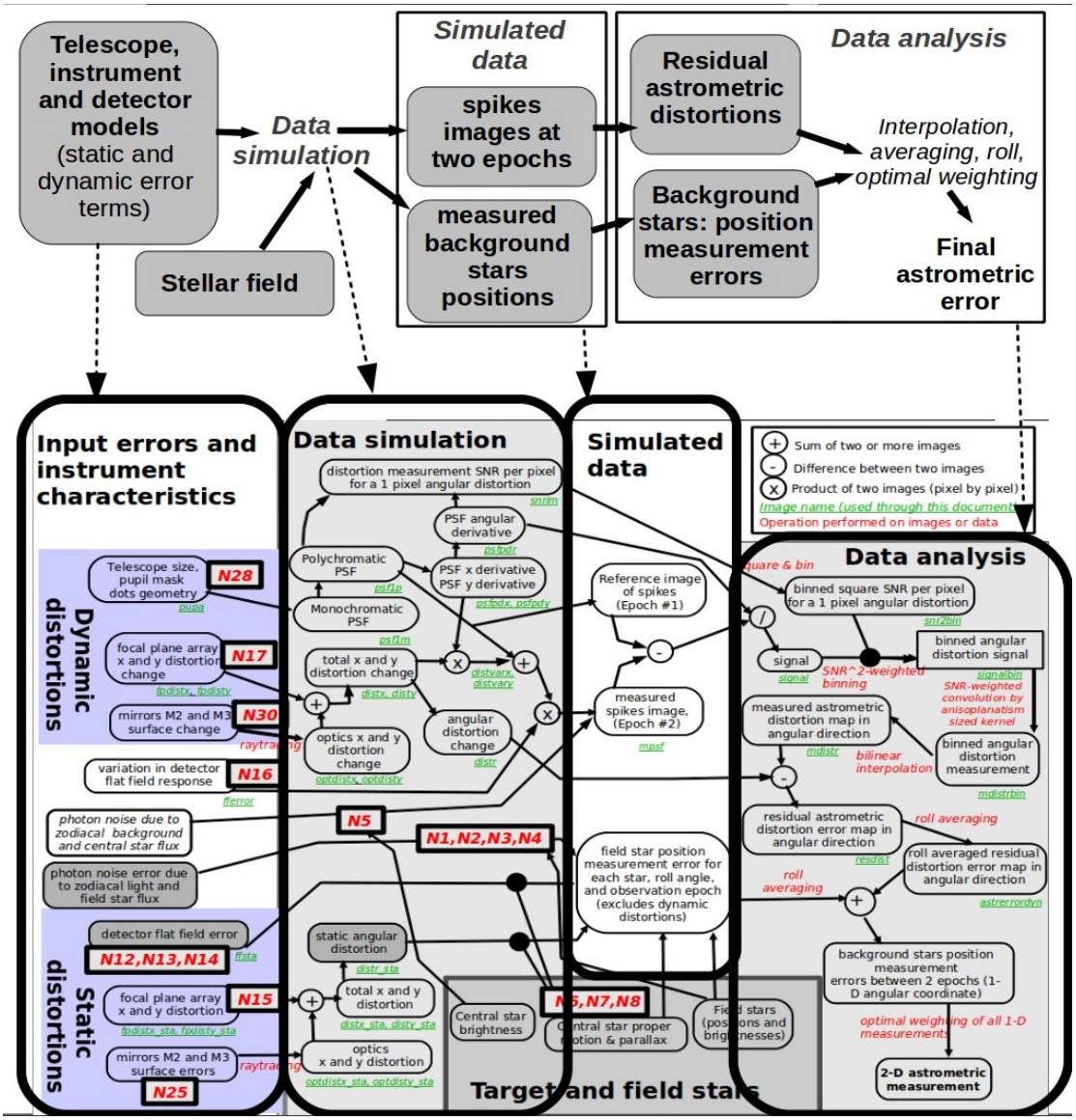

Figure 3. Numerical simulation overview: overview (top) and detailed step-by-step descrip-tion (bottom). The data acquired by the wide field camera is first simulated, including relevant sources of error. Images of the diffraction spikes and position measurement for the background stars are computed separately. The right part of the figure shows how the simulated data (or actual data from a mission) is analyzed to produce the 2-D astrometric measurement.

An end-to-end model of a DPT system using a wide-field 1.4 m diameter telescope was created to estimate the astrometric precision of the technique. A simplified block diagram of the model is shown in figure 3. Details of the numerical simulation can be found in a separate publication[ref], and we only recall here significant findings. The simulation used a 0.2 deg diameter field (0.03 deg^2) to keep computing requirements modest, and a 0.58 uas measurement precision per axis was obtained for the 2 day observation considered. The key findings are:

1. With the assumptions made for the numerical simulation, a 0.3 deg^2 field of view is required on the 1.4 m telescope considered to measure masses of planets with a 0.1 M_{Earth} precision for a 3 year mission.
2. Stars with apparent magnitudes between m_V=18 and m_V=20 contribute the most to the final measurement (for the galactic pole field case). Brighter stars are not sufficiently numerous to average down systematic errors (small scale distortions, detector defects), while fainter stars do not have sufficient combined flux to obtained a precise measurement.
3. The final astrometric measurement precision is quite robust against increased levels of instrument noise, as fainter and more numerous stars can be selected to average down instrumental noise with little impact on the final performance. For example, doubling the amplitude of all instrumental errors (distortions, detector defects) only increases the final astrometric measurement error by 23%.

The two last results are illustrated in figure 4, which shows the contribution of each background star in the field to the final astrometric measurement. For stars brighter than m_V=18, systematics dominate the error, while for fainter stars, photon noise dominates the error.

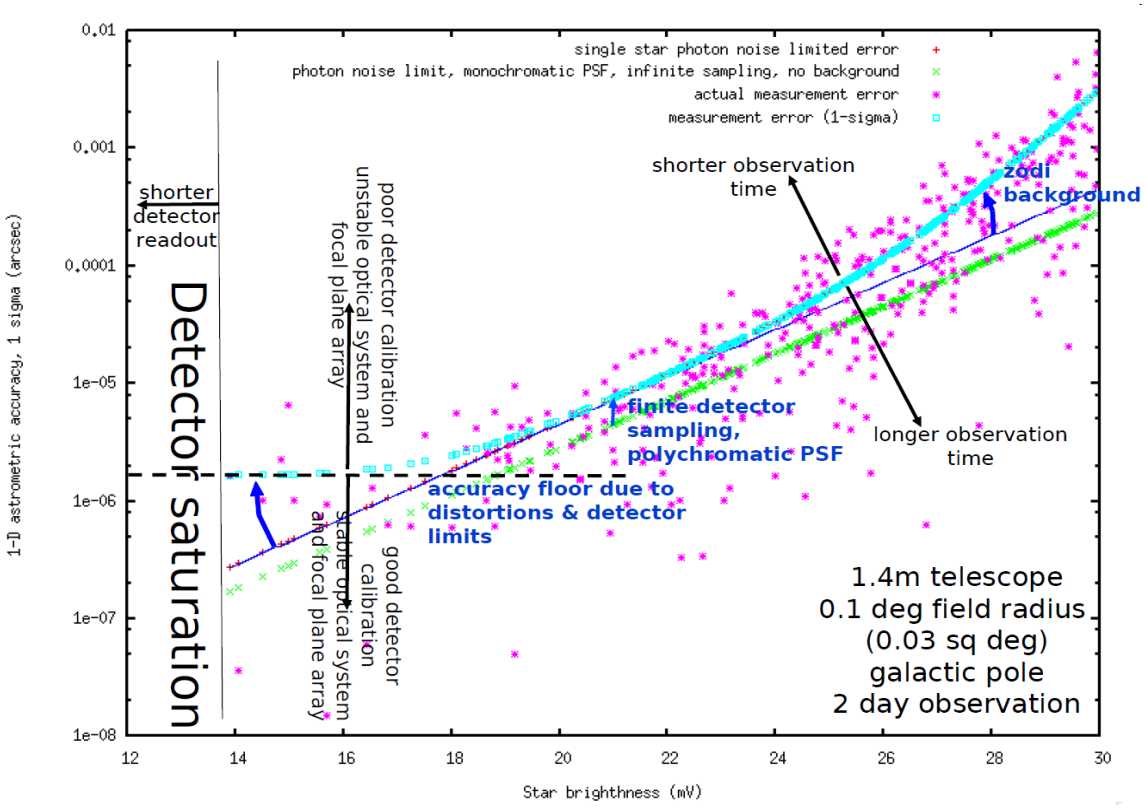

Figure 4. Contribution of each field star to the final astrometric measurement (single epoch observation).

3.2 Precision as a function of Telescope Size and Field of View

The numerical model described in the previous section can be used to explore other telescope diameter and field of view choices for the design. Results of this investigation are shown in table 2, and illustrate the steep improvement in astrometric measurement precision with increased telescope aperture.

Table 2. Expected single measurement astrometric accuracy as a function of telescope diameter and field of view (Galactic pole pointing, 2 day integration).

Telescope diameter	0.03 deg^2 (diam=0.2 deg)	0.1 deg^2 (diam=0.36 deg)	0.3 deg^2 (diam=0.6 deg)	1.0 deg^2 (diam=1.1 deg)
1.0 m	0.99 μas	0.54 μas	0.31 μas	0.17 μas
1.4 m	0.62 μas	0.34 μas	0.20 μas	0.11 μas
2.0 m	0.38 μas	0.21 μas	0.12 μas	0.066 μas
2.8 m	0.24 μas	0.13 μas	0.076 μas	0.041 μas
4.0 m	0.24 μas	0.081 μas	0.047 μas	0.026 μas
5.7 m	0.24 μas	0.050 μas	0.029 μas	0.016 μas
8.0 m	0.24 μas	0.032 μas	0.019 μas	0.010 μas

4. COMBINED ASTROMETRY, CORONAGRAPHY AND DEEP WIDE FIELD IMAGING

4.1 Simultaneous measurements

The DPT concept allows simultaneous coronagraph imaging of planets around the target star, astrometric measurement of the target star's position on the sky, and deep wide field imaging. These measurements do not negatively impact each other:

- Since the grid of dots on the primary mirror is regular, it does not contain low spatial frequencies, and therefore does not diffract light within the inner coronagraph field. The innermost edge of the spikes is at about 10 arcsec from the optical axis. The only effect of the primary mirror dots, as seen by the coronagraph, is a slight loss of throughput due to the light blocks or diffracted.
- The spikes are too faint (approximately 1e-8 of the peak star surface brightness) to negatively impact wide field imaging. Even when the telescope were pointed at Sirius (m_V=0), the additional background due to the central star would be smaller than the zodiacal light level over 95% of the field.

4.2 Detection and characterization of exoplanets

Simultaneous coronagraphic observation and astrometric measurement of the same target star allows robust identification of planets orbits and masses, even in multiple planets systems where coronagraphy-only or astrometry-only measurements may be ambiguous. To illustrate the complementarity of astrometric and coronagraphic measurements, and the value of performing both measurements, we have simulated the observation of a 3-planet system under two different mission scenarios:

• Astrometric mission: One observation is performed every month, with an 0.2 μas precision per axis.

• Astrometry + coronagraphy mission: Every two months, an astrometric measurement at the 0.2 μas precision per axis is performed, simultaneously with a coronagraphic observation.The planet positions are measured to 0.0088 arcsec precision per axis only when outside the coronagraph's IWA.

Direct comparison between the two scenarios is shown in figures 5 and 6. More detailed about this simulation will be published in an upcoming paper[3].

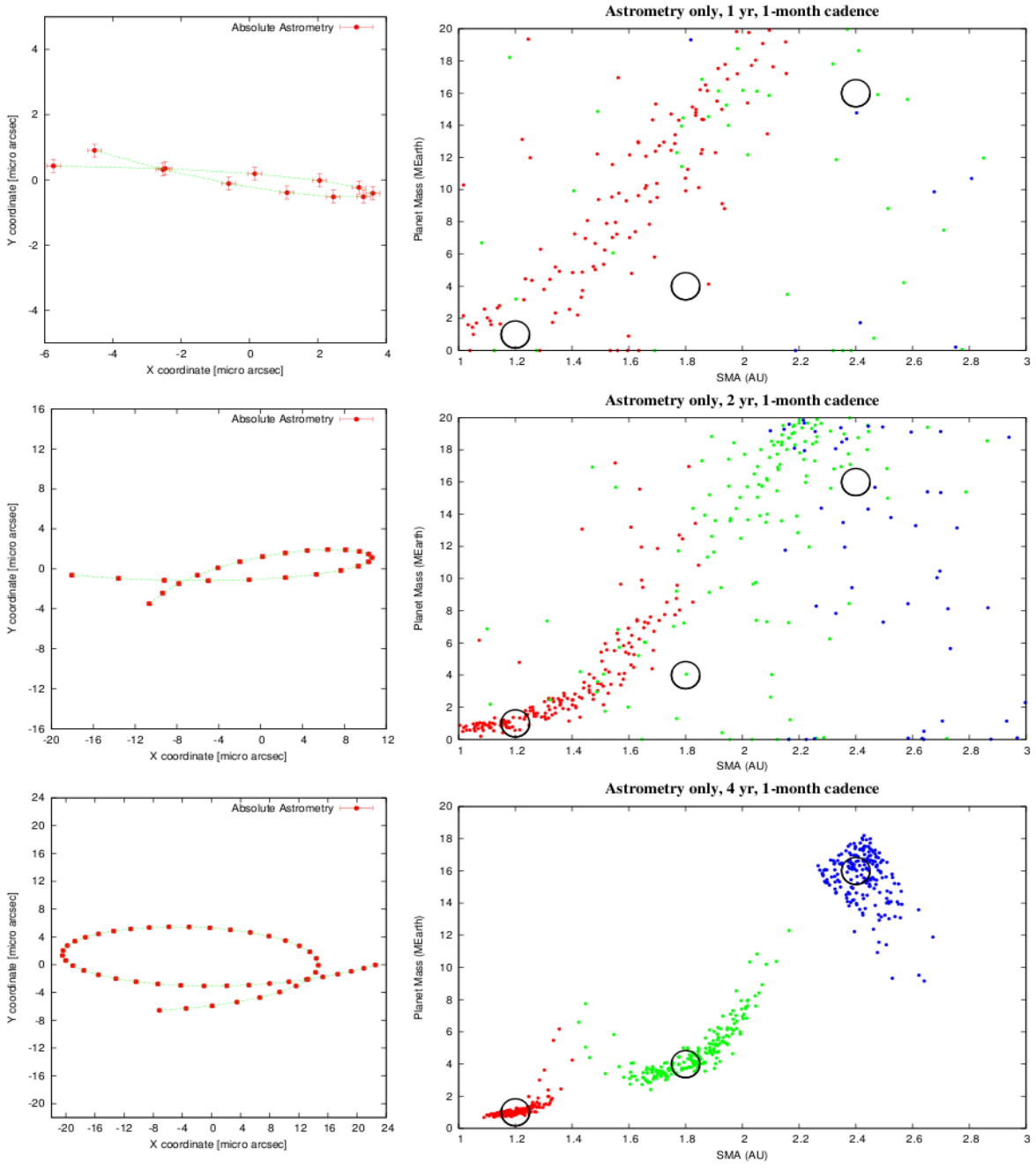

Figure 5. Result of the astrometry mission scenario, observing a 3 planet system around a Sun like star at 6pc. Values to be measured are shown on the left with measurement error bars (1-σ). 200 realizations of the observations are simulated, and the best 3-planet solution is shown on the right for each simulation in the semi-major axis - mass plane. Total mission duration is increased from top to bottom, from 1-year to 4-year. The 3 dark circles indicate the actual configuration for the 3-planet system. The initial starting point is the same for all scenarios: the first six absolute astrometry values are identical in all cases. However, the astrometric values shown in the left panel are corrected for uniform drift (proper motion) during the measurement period, resulting in different shapes and amplitude for the part of the astrometry trajectory curves common to all scenarios (first year).

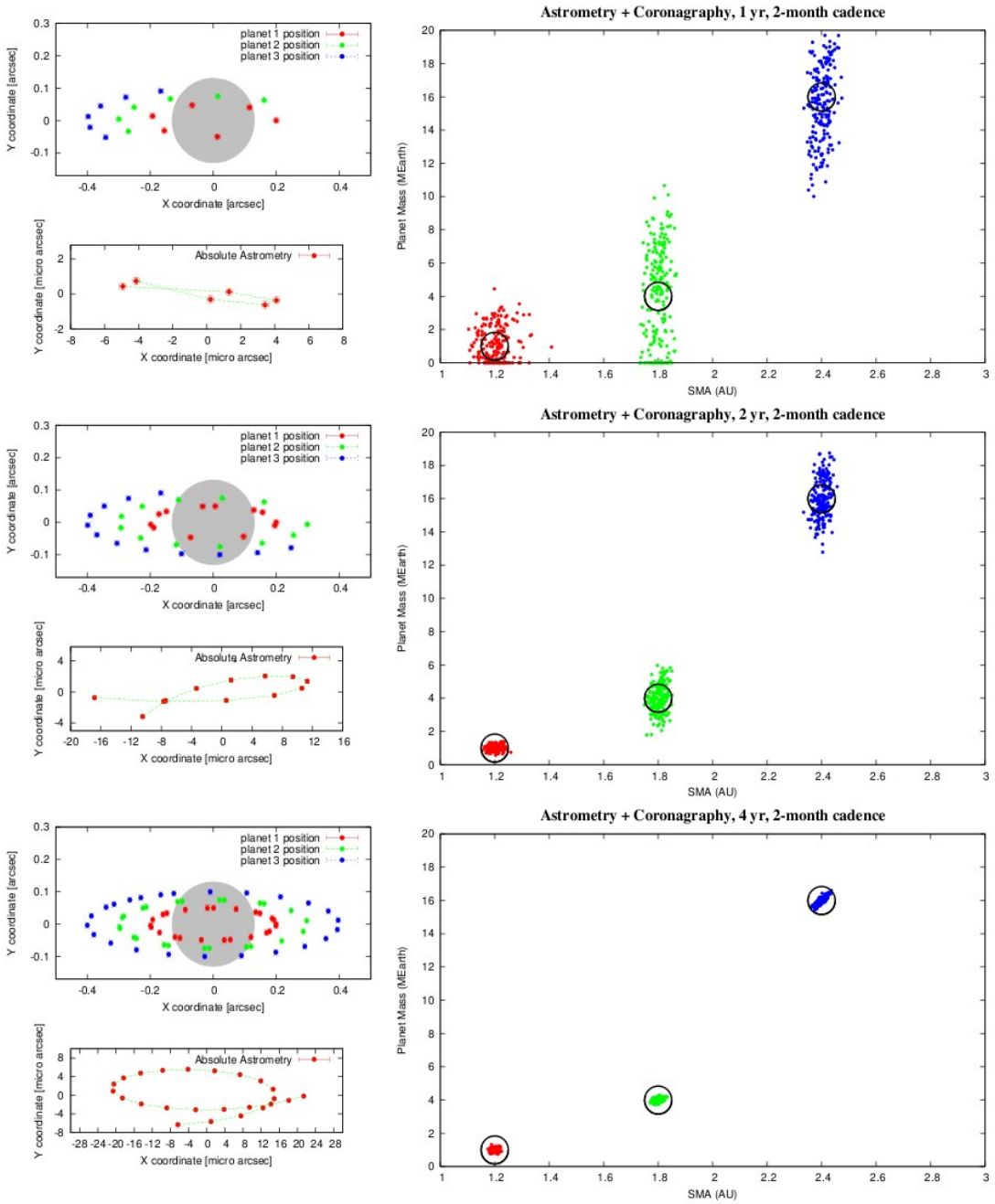

Figure 6. Result of the astrometry + coronagraphy mission scenario, observing a 3 planet system around a Sun like star at 6pc. Values to be measured are shown on the left with measurement error bars (1-σ). 200 realizations of the observations are simulated, and the best 3-planet solution is shown on the right for each simulation in the semi-major axis (x axis) - mass (y axis) plane. Total mission duration is increased from top to bottom, from 1-year (top) to 4-year (bottom). The grey disk indicates the blind area (within coronagraph inner working angle) for the planet-to-star relative astrometry measurements. The 3 dark circles indicate the actual configuration for the 3-planet system.

5. CONCLUSIONS AND FUTURE WORK

The diffractive pupil telescope (DPT) design allows simultaneous deep wide field imaging, coronagraphic imaging and astrometric mass determination of exoplanets around nearby stars. We have shown and quantified in both this paper and our previous publication that the measurements can be performed without impacting each other's performance: the coronagraphic and deep wide field observations are not significantly affected by the presence of dots on the primary mirror. The potential cost and complexity saving offered by combining three separate missions into one observatory could be significant, and we are thus currently evaluating the feasibility and performance of this concept through both simulations and laboratory demonstrations.

A laboratory testbed for the technique has been constructed at the University of Arizona, and is validating the principles of the concept, showing that astrometric distortions can be accurately measured by the diffraction spikes. A separate experiment was conducted at NASA Ames to validate the technique's compatibility with coronagraphic imaging. Both activities are described in a separate paper in this volume[2]. Use of the technique from the ground is also considered[4].

ACKNOWLEDGMENTS

This work is supported by the National Aeronautics and Space Administration (NASA) under an Astronomy and Physics Research and Analysis (APRA) grant.

REFERENCES

[1] Guyon, O., Ammons, S. M., Bendek, E. A., Eisner, J. A., Angel, R. P., Woolf, N. J., Milster, T. D., Shao, M., Shaklan, S., Levine, M., Nemati, B., Pitman, J., Woodruff, R. A., and Belikov, R., "High precision astrometry with a diffractive pupil telescope", ApJS, 200, 11 (2012)

[2] Bendek, E. A., Ammons, S. M., Belikov, R., and Pluzhnik, E. "High precision astrometry laboratory demonstration for exoplanet detectionusing a diffractive pupil," Society of Photo-Optical Instrumentation Engineers (SPIE) Conference Series 8842 (2012)

[3] Guyon, O., Eisner, J. A., Angel, R., Woolf, N. J., Bendek, E. A., Milster, T. D., Ammons, S. M., Shao, M., Shaklan, S., Levine, M., Nemati, B., Martinache, F., Pitman, J., Woodruff, R. A., Belikov, R., "Simultaneous Exoplanet Characterization and Deep Wide Field Imaging with a diffractive pupil telescope", ApJ Supplements, submitted (2012)

[4] Ammons, S. M., Bendek, E. A., Guyon, O., "Microarcsecond relative astrometry with MCAO using a diffractive mask, " Society of Photo-Optical Instrumentation Engineers (SPIE) Conference Series 8847 (2012)